International Journal of Pharmaceutics 434 (2012) 460–467

Contents lists available at SciVerse ScienceDirect

International Journal of Pharmaceutics

journal homepage: www.elsevier.com/locate/ijpharm

Pharmaceutical Nanotechnology

Evaluation of surface deformability of lipid nanocapsules by drop tensiometer technique, and its experimental assessment by dialysis and tangential flow filtration

Samuli Hirsjärvi*, Guillaume Bastiat, Patrick Saulnier, Jean-Pierre Benoît

LUNAM Université, Université d'Angers, INSERM U1066, Angers, France

ARTICLE INFO

Article history:
Received 2 May 2012
Received in revised form 4 June 2012
Accepted 5 June 2012
Available online 12 June 2012

Keywords:
Lipid nanocapsules
Drop tensiometer
Dialysis
Tangential flow filtration
Rheology

ABSTRACT

Deformability of nanoparticles might affect their behaviour at biological interfaces. Lipid nanocapsules (LNCs) are semi-solid particles resembling a hybrid of polymer nanoparticles and liposomes. Deformability of LNCs of different sizes was modelled by drop tensiometer technique. Two purification methods, dialysis and tangential flow filtration (TFF), were applied to study experimental behaviour and deformability of LNCs in order to evaluate if these properties contributed to membrane passing. Rheological parameters obtained from the drop tensiometer analysis suggested decreasing surface deformability of LNCs with increase in diameter. Dialysis results showed that up to 10% of LNCs can be lost during the process (*e.g.* membrane accumulation) but no clear evidence of the membrane passing was observed. Instead, LNCs with initial size and size distribution could be found in the TFF filtrate although molecular weight cut-off (MWCO) of the membrane used was smaller than the LNC diameter.

1. Introduction

Extensive studying of nanosized particles during the last decades have resulted in drug delivery systems that protect the active substance, improve solubility and target the drug to specific tissues in the body (Farokhzad and Langer, 2009). Areas such as cancer therapy benefit from these advances (Hirsjärvi et al., 2011). Most of the nanosized drug carrier particles consist of polymer or lipid materials (Kumari et al., 2010; Müller et al., 2011; Torchilin, 2005,2007). Lipid nanocapsules (LNCs) are synthetic particles whose structure can be characterized as a hybrid between polymer nanoparticles and liposomes (Heurtault et al., 2001, 2002a). They consist of low-toxicity materials (PEGylated surfactant, lecithin, triglycerides) and their fabrication, based on low-energy organic solvent-free phase inversion process, can be easily scaled up. Moreover, their size can be tuned within the range of 20–100 nm (Heurtault et al., 2003b). LNCs have been applied *e.g.* in the delivery of cancer therapeutics (Cirpanli et al., 2011; Lacoeuille et al., 2007; Peltier et al., 2006) and other drug molecules (Lamprecht et al., 2004), macromolecules such as siRNA and DNA (Morille et al., 2010, 2011), and in radiotherapy (Allard et al., 2008; Vanpouille-Box et al., 2011a,b).

Apart from size, surface charge and hydrophilicity, elasticity and shape are less studied parameters that can have a profound influence on the nanoparticle fate *in vivo* (Decuzzi et al., 2010; Longmire et al., 2011; Perry et al., 2011). In fact, elasticity is reported to have an effect on the biodistribution and membrane passing capacity of nanoparticles (Arkhangelsky et al., 2011; Christian et al., 2009). For example, renal clearance of flexible dendrimers (~15 nm) was more pronounced compared to "hard" dendrimers of the same size (renal clearance cut-off ~10 nm) (Longmire et al., 2011). Elasticity is also considered as an important factor in the evaluation of toxicology of nanomaterials (Elsaesser and Howard, 2012). Elasticity might also be related to the mobility of the molecular chains on the nanoparticle surface, thus affecting the uptake by the mononuclear phagocyte system (MPS) (Vonarbourg et al., 2006a).

Due to their semi-solid hybrid structure, shell of an LNC can be expected to express dynamic behaviour and elasticity. These properties have been studied by interfacial deposition technique with the help of Langmuir balance (Heurtault et al., 2003a; Minkov et al., 2005a,b). Comportment of Solutol®, the main surfactant on the LNC shell, on an oil–water interface has been studied using drop tensiometer technique (Heurtault et al., 2002b). The results demonstrated, indeed, the dynamic nature of LNCs (elastic behaviour upon compression) but also their structural stability.

* Corresponding author at: INSERM U1066, IBS-CHU Angers, 4 rue Larrey, 49933 Angers Cedex 9, France. Tel.: +33 2 44 68 85 39; fax: +33 2 44 68 85 46.
E-mail addresses: samuli.hirsjarvi@univ-angers.fr (S. Hirsjärvi), guillaume.bastiat@univ-angers.fr (G. Bastiat), patrick.saulnier@univ-angers.fr (P. Saulnier), jean-pierre.benoit@univ-angers.fr (J.-P. Benoît).

0378-5173/$ – see front matter © 2012 Elsevier B.V. All rights reserved.
http://dx.doi.org/10.1016/j.ijpharm.2012.06.019

In vitro, regardless their sizes in the range of 20–100 nm, LNCs are rapidly internalized by cells (*e.g.* macrophages, different cancer cells) (Paillard et al., 2010; Vonarbourg et al., 2006b). Smaller LNCs (20 nm) were observed to escape lysosomes more efficiently than the bigger ones (Paillard et al., 2010). Passage of LNCs across a model intestinal barrier has been shown to be size-independent (Roger et al., 2009). Increasing LNC size (20–100 nm) resulted in increased activation of the complement system (Vonarbourg et al., 2006b). However, these previous LNC studies have not elucidated the role of the possible particle deformability on the biological behaviour.

Therefore, in this study, to make next step towards deformability evaluation of LNCs, characterization of rheological properties of oil-in-water drops mimicking LNCs of different sizes was performed by drop tensiometer. Drop tensiometer technique has been used previously to study rheology of different molecules such as lipids (Anton et al., 2007; Li et al., 1999; Wüstneck et al., 1999b), proteins (Benjamins et al., 1996; Liu et al., 2011; Wüstneck et al., 1999a), polyoxyethylene-type and other surfactants (Ramírez et al., 2011; Santini et al., 2007), and biological samples (serum) (Kazakov et al., 2008) on diverse interfaces. Deformability of LNCs was then evaluated experimentally according to their behaviour during purification by dialysis and tangential flow filtration (TFF). Dialysis is a widely used classic method to remove impurities and excess molecules. TFF is a less-used alternative purification method for nanoparticle dispersions (Dalwadi et al., 2005; Dalwadi and Sunderland, 2007, 2008; de Jaeghere et al., 1999; Hirsjärvi et al., 2009, 2010; Limayem et al., 2004; Saez et al., 2000; Sweeney et al., 2006). Particularly, loss of LNCs during these processes was assessed.

2. Materials and methods

2.1. Materials

Solutol® HS15 (PEG 660 12-hydroxystearate, $M_W \sim 870$ Da) (BASF, Ludwigshafen, Germany), Labrafac® WL 1349 (caprylic/capric acid triglycerides) (Gattefossé S.A., Saint-Priest, France), Lipoid® S75-3 ($M_W \sim 780$ Da) (Lipoid GmbH, Ludwigshafen, Germany), NaCl (Prolabo VWR International, Fontenay-sous-Bois, France) and MilliQ185 water (Waters, Saint-Quentin-en-Yveline, France) were used in LNC formulation. 3,3-Dioctadecyloxacarbocyanine perchlorate (DiO) was from Invitrogen (Cergy-Pontoise, France). All other used reagents were of analytical grade.

2.2. Methods

2.2.1. Lipid nanocapsule (LNC) preparation and characterization

LNCs were prepared by the phase inversion temperature method described by Heurtault et al. (2003b). A mixture of Solutol®, Lipoid®, Labrafac®, NaCl and water was heated to 85 °C at a rate of 5 °C/min followed by cooling at the same rate to 65 °C. This cycle was repeated twice. During the last decrease of temperature, at 78 °C (during the phase inversion zone), the system was diluted with cold (4 °C) water leading to formation of stable LNCs. Size of LNCs (25, 50, 100 nm) was adjusted by changing the proportions of the components (Table 1). Fluorescent dye (DiO) was dissolved in acetone and added in the LNC preparation vial. Acetone was evaporated before addition of the components of the LNCs. Final concentration of DiO was 3 mmol/L/total Labrafac® amount (LNC core).

Size distributions and zeta (ζ) potentials of LNCs were determined with a Zetasizer ZS (Malvern, Worcestershire, UK). Particle sizing was based on photon correlation spectroscopy (PCS); the results were analysed by CONTIN algorithm and the sizes were presented based on the volume distributions together with polydispersity indices (*PdIs*). Electrophoretic mobilities were converted to ζ-potentials using Smoluchowski's equation.

2.2.2. Evaluation of the LNC composition

Quantities of LNCs (of different sizes) were estimated according to following equation:

$$x = \frac{3m}{\rho\pi 4r^3} \quad (1)$$

where m and ρ are mass (Table 1) and density (945 g/L) of Labrafac®, respectively, and x is the quantity of LNCs. Molar-% proportions of Lipoid® and Solutol® in an LNC formulation were calculated from the total quantity of these components (Table 1) used. Quantity in moles of the components on the surface of a single LNC was

$$\frac{n(\text{total})}{\text{LNC}} = \frac{n(\text{Solutol}^{®}) + n(\text{Lipoid}^{®})}{x} \quad (2)$$

$$\frac{n(\text{total})}{A} = \frac{n(\text{total})/\text{LNC}}{4\pi r^2} \quad (3)$$

where x is the quantity of LNCs, and A and r the surface area and radius of a single LNC, respectively. Previously, the totality of Solutol® and Lipoid® are shown to participate in the particle formation (unpublished data). n(total)/A was used to determine the amounts of Lipoid® and Solutol® on the surface of a model Labrafac® drop that was used in the drop tensiometer studies. Volume of the Labrafac® drop was 5 μL and the surface area of such a drop was evaluated to be about 12.5 mm^2 (the area is smaller than that of a 5 μL drop because of space occupied by the gauge).

2.2.3. Rheology by drop tensiometer technique

Rheological behaviour of an oil–water interface (Labrafac®-water) containing different quantities of Lipoid® and Solutol®, respectively, was measured by a drop tensiometer (Tracker, ITConcept, Longessaigne, France). Lipoid® and Solutol® concentrations were calculated according to their mol% in the surface of LNCs (Table 2). The tested concentrations varied from 100% Solutol® (0% Lipoid®) to 100% Lipoid® (0% Solutol®). *n/A* concentration of LNC 50 nm (Table 2) was used for the calculation of the total Lipoid® + Solutol® concentration (except the model drops for LNC 25 and 100 nm). A 5 μL (~12.5 mm^2) rising drop of Labrafrac® was formed using an Exmire microsyringe and a gauge (Prolabo, Paris, France) into a glass vial filled with the aqueous phase. The axial symmetric shape (Laplacian profile) of the drop was analysed using a camera connected to a computer. From the analysis of digital image with Laplace equation integration of the drop profile, the interfacial tension and surface area could be simultaneously calculated and recorded in real time. Volume was controlled by the motor operating the microsyringe. In order to let Lipoid® and Solutol® adsorb on the interface, the drop was equilibrated for 16 h (at 25 °C) keeping the surface area constant with the help of the syringe motor. At the end of the equilibration time, equilibrium surface tension was registered. To obtain the rheological parameters, the drop was then subjected to harmonic (sinusoidal) surface area alterations. Amplitude of the sinusoids was 0.3 μL (sinusoids were performed by the volume change because of higher precision) corresponding to about 5% change in the surface area. Magnitude of such surface area change enabled retaining linear conditions. Periods (pulsations, ω) of the sinusoids ranged from 3 to 300 s corresponding to a rad/s range 2.09–0.02. Observed alterations in surface tension for each pulsation were treated by a harmonic analysis (Windrop software, ITConcept, Longessaigne, France) that allowed calculation of the parameters G' (elasticity real part) and G'' (elasticity imaginary part), characteristic for the rheological comportment of the interface (Saulnier et al., 2001).

Table 1
Composition of LNCs of different sizes. Volume of the cold (4 °C) water added during the phase inversion zone was 4.2 mL leading to a total volume of about 5.7 mL.

	Solutol® (mg)	Lipoid® (mg)	Labrafac® (mg)	NaCl (mg)	Water (mg)
LNC 25 nm	645	25	282	30	685
LNC 50 nm	282	25	343	30	987
LNC 100 nm	161	25	403	30	1048

Table 2
Particle quantities and theoretical amounts of the tensioactive components Lipoid® and Solutol® on the LNC surface.

	Particle quantity[a]	n(Solutol® + Lipoid®)/A (mol/m^2)	Lipoid® (%)	Solutol® (%)
LNC 25 nm	7.12×10^{16}	8.63×10^{-6}	4	96
LNC 50 nm	5.54×10^{15}	8.19×10^{-6}	9	91
LNC 100 nm	8.14×10^{14}	8.50×10^{-6}	15	85

[a] Total particle quantity resulting from a formulation with the amounts of the components announced in Table 1.

The current model used to simulate the rheological characteristics of an interface with sinusoidal pulsations is a parallel association of a Maxwell liquid and a perfect elastic solid (Hooke's law) (Saulnier et al., 2001). The perfect elastic solid reflects the pure elasticity of a monolayer with cohesive interactions between amphiphilic molecules at the interface. This phenomenon corresponds to the rheological parameter E_e, the elastic compliance (long range organization of the interface and the interactions between the interfacial molecules). The Maxwell liquid reflects the energetic dissipation of the monolayer, *i.e.* the displacements of the amphiphilic molecules from/to the monolayer due to compression/expansion, respectively. This dissipative phenomenon corresponds to two rheological parameters: E_{ne} (elasticity component) and τ (in relation with the viscosity component). E_{ne} is linked to molecular interactions between the amphiphilic molecules and the aqueous or the lipophilic phase; τ stands for the time of the interface to reach a new equilibrium energetic state after a perturbation (compression/expansion). With this approach, G' and η (viscosity) are expressed as a function of ω (duration range of the sinusoidal pulsations):

$$G'(\omega) = E_e + E_{ne}\frac{\omega^2\tau^2}{1+\omega^2\tau^2} \quad (4)$$

$$\eta(\omega) = \frac{G''(\omega)}{\omega} = E_{ne}\frac{\tau}{1+\omega^2\tau^2} \quad (5)$$

Fortran program for experimental curve fitting, based on a traditional optimization method called simulated annealing, with a 0.95 tolerance was used. The parameters E_e, E_{ne} and τ, elastic component, dissipative component and relaxation time, respectively, were optimized independently ($G'(\omega)$ or $\eta(\omega)$) and simultaneously ($G'(\omega)$ and $\eta(\omega)$). Parameters presented in this study are results of means and standard deviations of the various optimizations.

2.2.4. Dialysis and tangential flow filtration (TFF)

LNCs were dialysed with 3.5 or 15 kDa MWCO (molecular weight cut-off) Spectra/Por regenerated cellulose membranes (Spectrum Laboratories, Inc., Breda, The Netherlands) overnight. The dialysed volumes were 500 μL and the external medium was 800 mL.

TFF was performed with a continuous diafiltration mode (the dispersion volume remained the same during filtration) using a Minimate™ TFF System and a Capsule with Omega ^{TI} 3 K or 10 K MWCO Membrane (Pall Corporation, Ann Arbor, USA) run by a peristaltic pump. Principle of TFF is presented in Fig. 1. The flow rate was 40 mL/min, filtration rate 1–2 mL/min and operating pressure 10–20 psi. The LNC dispersion volume was 10 mL (concentration 20 mg/mL) and the volume of water used in purification was 100 mL. 5 mL fractions of filtrate were collected. The filtration capsule was washed with 0.5 mol/L NaOH and water after each filtration as recommended by the fabricant.

Count rate (kilo counts per second, kcps) expresses the scattering intensity detected during a PCS analysis, *i.e.* the sample concentration. Theoretical particle concentrations were evaluated from the PCS data of the dialysed LNCs and the TFF filtrate fractions by dividing measured count rate by attenuation factor. The obtained derived count rate (DCR) allowed comparison of the dialysed LNC (taking into account the eventual volume increase) and the TFF fractions with the initial LNC dispersion (% LNC after dialysis or % LNC in a fraction of the initial LNC concentration). Similarly, fluorescence intensities of the dialysed LNCs were measured before and after dialysis, and also fluorescence intensities of the TFF fractions *vs.* the TFF feed LNC dispersion (Fluoroskan Ascent FL, Thermo Scientific, Waltham, USA), in order to evaluate the quantity of LNC lost during these processes.

3. Results and discussion

3.1. LNC preparation and characterization

Size as well as size distribution profiles revealed the homogeneous nature of LNCs prepared by the phase inversion temperature method (Table 3). ζ-Potentials of the LNCs were slightly negative which is assumed to originate from PEG groups at the surface forming dipoles able to interact with counterions or water dipoles (Vonarbourg et al., 2005). As reported earlier, encapsulation of the lipophilic fluorescent dye (DiO) did change neither size nor ζ-potential profile when compared to the empty LNC (Morille et al., 2010; Zou et al., 2008).

The structure of LNCs is expected to be the following: an oily liquid core corresponding to free Labrafac® that is surrounded by a tensioactive rigid shell made of a mixture of Lipoid® and Solutol® (Heurtault et al., 2002a). Because of lipophilic nature of Lipoid® and hydrophilic nature of Solutol®, the former is anchored in the oily phase (and not present in the outer parts of the LNC shell), whereas the latter orientates towards the aqueous phase (Heurtault et al., 2003a; Vonarbourg et al., 2005). Lipoid® provides stability to the LNC structure, and in fact, LNCs prepared without this component dissociate rapidly: this has been proven by a Langmuir balance model (Minkov et al., 2005a,b) and also in practice (Vonarbourg et al., 2005).

When the particle quantity of LNCs was evaluated by Eq. (1), the amount of LNC 25 nm was found to be about 13-fold higher than

Table 3
Size and ζ-potential of LNCs of different sizes.

	Size (nm)	*PdI*	ζ-potential (mV)
LNC 25 nm	25 ± 2	0.07	−2 ± 2
LNC 50 nm	50 ± 1	0.03	−3 ± 1
LNC 100 nm	99 ± 1	0.05	−4 ± 2

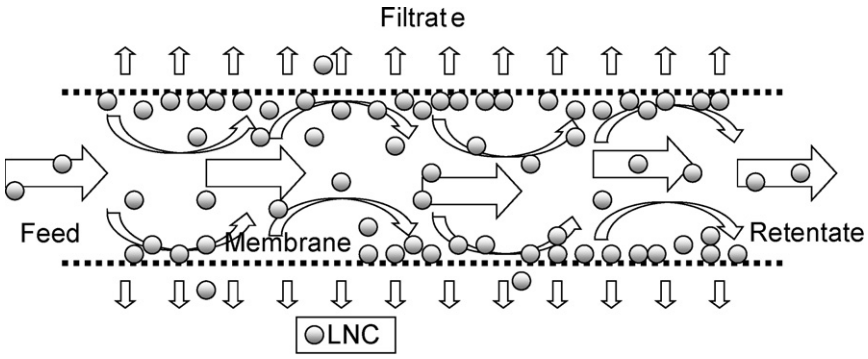

Fig. 1. Principle of TFF. Particle dispersion flows tangentially to the membrane, creating a pressure difference across the membrane (with the help of a peristaltic pump and regulation of the filtrate formation rate by clamps). Because of the applied pressure and device geometry, the dispersion flow becomes turbulent near the membrane surface. This reduces cake formation on the membrane.

that of LNC 50 nm, and the amount of LNC 50 nm about 7-fold higher than that of LNC 100 nm (Table 2). Despite this decrease in the particle quantity by the increase in size, surface densities of Lipoid® and Solutol® on a single LNC surface (n(total)/A) (Eqs. (2) and (3)) remained in the same range within the all three sizes (Table 2). When the particle formation is spontaneous (phase inversion), the particle size depends on the quantities of the components: oil, water and the surfactants. Therefore, the differences between the surface compositions were found in the proportions of Lipoid® and Solutol®: increasing the LNC size, the Solutol® quantity decreased while the Lipoid® quantity increased.

3.2. Rheology by drop tensiometer technique

The particle size effect, *i.e.* the change of the proportions of the LNC components on the particle structure deformability, was studied by drop tensiometer. Simulation of LNCs by this technique was based on the adsorption of Lipoid® and Solutol® on the Labrafac®-water interface. Concentrations of Solutol® in water and Lipoid® in Labrafac® were determined directly from their theoretical amounts on the surface of the model 12.5 mm^2/5 μL drop and converted to mol/L. The concentrations thus obtained (2.16×10^{-5}, 2.05×10^{-5}, and 2.13×10^{-5} mol/L for 25, 50, and 100 nm LNCs, respectively) provided sufficiently molecules for the interface adsorption, and, more importantly, the equilibrium interfacial tensions (γ) settled in the range of 9–10 mN/m which enabled successful execution of the sinusoids. As a comparison, previous studies have shown that a pseudo-CMC of Solutol® in water exists around 1×10^{-3} mol/L (Heurtault et al., 2002b). Such a concentration provides certainly excess of molecules for the surface adsorption, but with Lipoid®, low γ (2–3 mN/m) provoke drop ejection during the sinusoids.

γ of different Lipoid®/Solutol® compositions are presented as a Lipoid® concentration in Fig. 2. γ of Lipoid® 0%/Solutol® 0%, 22.6 ± 0.4 (=a drop of Labrafac® in water; not in Fig. 2) and Lipoid® 100%/Solutol® 0%, 20.3 ± 0.9, were clearly higher than γ of the other tested concentrations. Lipoid® alone did not act as an efficient tensioactive molecule. Due to this drop rigidity, sinusoid series including short periods could not be performed with these two reference concentrations (volume alterations did not produce tension changes that could have been treated successfully by the harmonic analysis). When Solutol® was included in the drops, γ decreased in the range of 9–10 mN/m, and the sinusoids could be performed with success. Slightly increasing tendency of γ was observed in the concentration range of simulated LNCs (4–15% Lipoid®): γ is expected to increase with LNC size. As the Lipoid® proportion was further increased (Lipoid® 50% and 75%), γ increased (10.6–13.0 mN/m) also indicating the stiffening effect of Lipoid® (Heurtault et al., 2003a; Minkov et al., 2005a,b; Vonarbourg et al., 2005).

At constant temperature and pressure, interfacial tension equals Gibbs free energy (ΔG) per surface area. Thus, in our concentration region of particular interest (4–15% Lipoid®), ΔG increased with decreasing Solutol® proportion at the interface. Based on this, it can be assumed that increase in LNC size, together with change of Lipoid® and Solutol® proportions, is accompanied by formation of an energetically less stable and less structured surface.

Rheological parameters E_e, E_{ne}, and τ as a function of Lipoid® proportion are summarized in Fig. 3. Generally, increase in E_e values means increasing elasticity whereas increase in E_{ne} means rigidity but molecules can leave the interface more easily after a

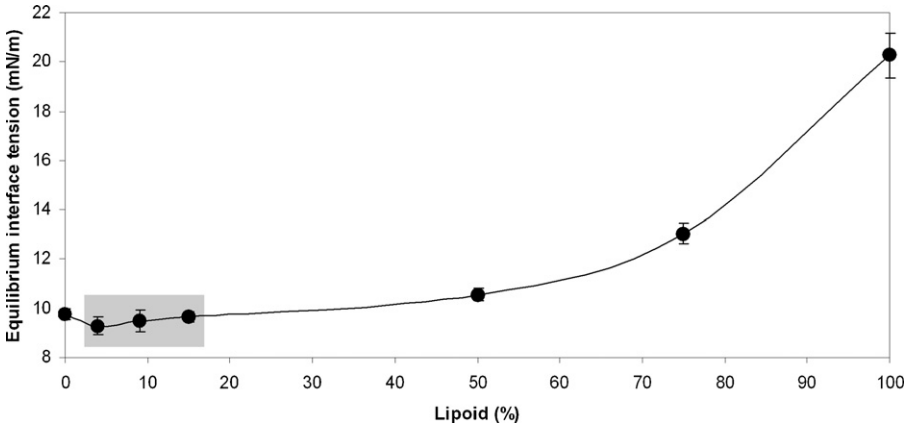

Fig. 2. Equilibrium interfacial tensions (γ) as a function of Lipoid® composition (0% Lipoid® = 100% Solutol® etc.). The range mimicking LNCs (25–100 nm) is highlighted by a grey rectangle.

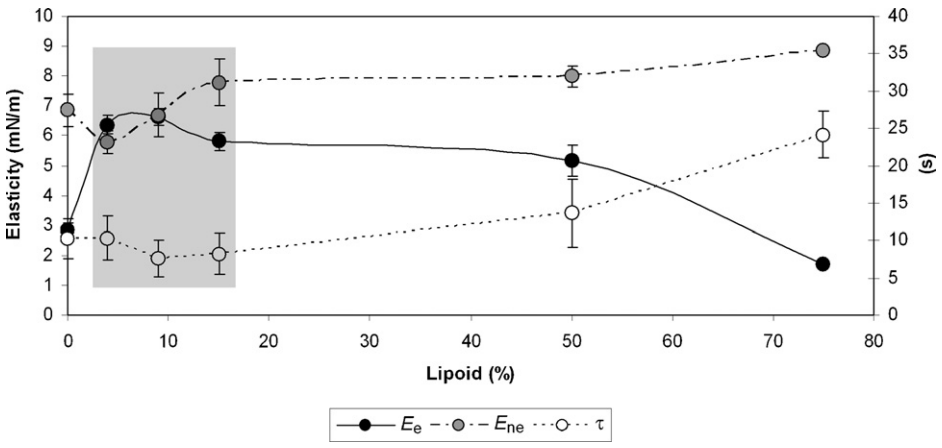

Fig. 3. Evolution of the rheological parameters E_e, E_{ne}, and τ as a function of Lipoid® proportion. The range mimicking LNCs (25–100 nm) is highlighted by a grey rectangle. Y-axis graduation on the left (mN/m) is for E_e, E_{ne}; graduation on the right (s) is for τ.

perturbation (Heurtault et al., 2003a; Saulnier et al., 2001). E_e/E_{ne} ratio for 100% Solutol® (0% Lipoid®) was low (0.4) indicating poor interfacial stability. This was in line with the previous studies reporting impossibility of preparing stable LNC without Lipoid® (Minkov et al., 2005a,b; Vonarbourg et al., 2005). Arriving at the concentration range of the simulated LNCs (4–15% Lipoid®), E_e/E_{ne} increased indicating stabilizing effect of Lipoid®. E_e/E_{ne} ratios in this concentration range showed a decreasing tendency: 1.1, 1.0, and 0.7 for 4%, 9%, and 15% of Lipoid®, respectively. These ratios suggested that the interface fluidity decreased with increasing Lipoid® concentration which might mean, correspondingly, decreasing particle surface deformability with LNC size increase. As the Lipoid® proportion was further increased, E_e/E_{ne} decreased being 0.6 and 0.2 for 50% and 75% Lipoid®, respectively, continuing the tendency of decreasing interfacial fluidity. Increasing amount of Lipoid® increased τ, which meant a longer relaxation time and was also in line with the E_{ne} tendency (more molecules could leave the interface and their return took longer time).

According to these results, it seems that a region existed where the interface was the most elastic (high E_e) and the most stable (low E_{ne}). Stable and monodisperse LNCs can be prepared in this region. Evolution of E_{ne} throughout the studied Lipoid®/Solutol® proportion range was similar to γ (Fig. 3). These results of rheological parameters are, thus, in line with the ΔG increase with LNC size. Formation of LNCs has been modelled previously with a feasibility diagram (Heurtault et al., 2003b), but it has not been linked to the rheological behaviour of a model interface.

Keeping the molecular concentrations the same, drop volume was increased from 5 to 10 μL in order to see if this volume increase could contribute to the LNC size *vs.* deformability evaluation. Nevertheless, the G' and G''/ω curves obtained from the harmonic analysis remained superimposable with the 5 μL curves (data not shown). If the size, *i.e.* the surface form, has an effect, it might appear only at nano-scaled surfaces. At least when using the drop tensiometer technique, the Lipoid®/Solutol® composition seemed to be more important than the surface form.

Overall, the obtained rheological parameters were in line with the previous study despite some experimental differences (Lipoid® included in the current study, different value extrapolation) (Heurtault et al., 2002b). Instead, comparison of the current results to the rheological parameters found in literature is challenging because of different interfaces and adsorbed molecules used, different experimental conditions (*e.g.* pulsation range), and differences in calculation approaches. However, studies with similar magnitudes were found. Real part G' values of the transfer function of a xanthan gum/sodium caseinate system on corn oil–water interface were about 2–15 mN/m which corresponded well with our values (Liu et al., 2011). In another study, dilatational elasticity (equilibrium elasticity) of Span™ 80 surfactant on paraffin oil–water interface was less than 10 mN/m over the studied concentration range (Santini et al., 2007).

Summarizing all this, the rheological results in this study support previous findings that the LNC surface presents certain fluidity/deformability with a sufficiently stable interface to form stable nanostructures (Heurtault et al., 2003a). It can also be assumed that deformation of LNCs is possible to some extent without destruction of the particle structure, and this deformability decreases with LNC size. Therefore, capacity of LNCs to pass membranes during purification processes was next studied experimentally.

3.3. Dialysis

LNCs of different sizes were dialysed in order to evaluate the quantity of particles lost during this purification process. Detection of the LNCs was based on the calculation of DCR and the measurement of fluorescence intensity of the LNC dispersion before and after dialysis. Regenerated cellulose membranes of two different MWCO were used: 3.5 kDa and 15 kDa.

Dialysis results are presented in Fig. 4. The DCR method proposed that about 93–95% of LNCs remained in their dispersion after dialysis. Using the smaller MWCO membrane, the average percentage of LNCs remaining after dialysis, evaluated by the fluorescence method, decreased from about 96 to 90% with the size increase from 25 nm to 100 nm. With the bigger membrane, the same decrease was from about 95–88%. However, these differences were not statistically significant. In earlier studies, decrease of radioactivity of a radiolabelled LNC 50 nm suspension was measured after a 2 h dialysis (Allard et al., 2008; Vanpouille-Box et al., 2011b). This shorter dialysis time (*vs.* 24 h in this study) resulted in 1.5–2.5% (relative) loss in radioactivity which can also be considered to result from particle loss.

Because of the tortuous nature of most membrane materials, such as regenerated cellulose or polyethersulfone, determination of the exact pore size is challenging (Sakai, 1994). However, mean pore size of 2.6 nm for a 10 kDa MWCO regenerated cellulose membrane (Zydney and Xenopoulos, 2007) and mode pore diameter 2.75–4.93 nm for a 20 kDa MWCO polyethersulfone membrane (Arkhangelsky and Gitis, 2008) have been reported. These pore sizes, obtained for comparable membranes as used in this study, are much smaller than the diameters of the LNCs dialysed (25–100 nm). Penetration of particles bigger than filtration

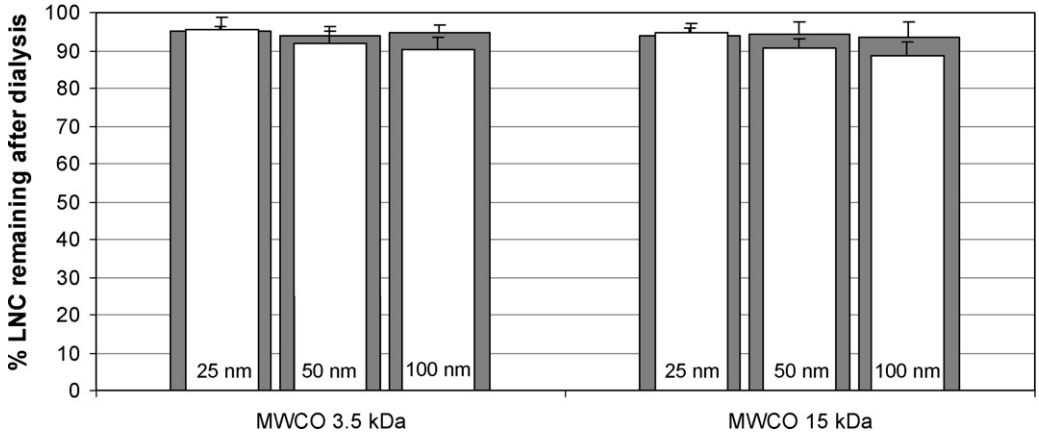

Fig. 4. Percentage of the LNC (25, 50, and 100 nm) quantity remaining in their dispersion after dialysis using two membrane MWCOs. The LNC quantity was evaluated by derived count rates (DCR, grey bars) and by fluorescence intensity (white bars). No statistical differences ($p < 0.05$ considered as significant, one-way ANOVA) were found between the LNCs of different sizes dialysed with the same membrane MWCO or between the two methods (DCR, fluorescence).

membrane pores has been observed *e.g.* in the case of water treatment from micro organisms (Arkhangelsky and Gitis, 2008; Urase et al., 1996) or when experimental membrane penetration of plasmid DNA was studied (Arkhangelsky et al., 2011). Proposed explanations for this included the presence of abnormally large pores not included in the announced pore size distribution, or mechanical defects due to membrane handling or sealing (Urase et al., 1996). On the other hand, change in the shape of the particles as they pass through the membrane has been described (Arkhangelsky et al., 2011). Pores have also been reported to undergo a pressure-induced enlargement when transmembrane pressure was increased during a filtration process (Arkhangelsky and Gitis, 2008). This phenomenon was obviously negligible in dialysis as the only driving force was concentration gradient. AFM observations have revealed that *e.g.* 20 kDa MWCO polyethersulfone membrane contains about 15–75 nm "valleys" that lead most probably to the pores (Arkhangelsky and Gitis, 2008). Therefore, the LNC loss during dialysis could be explained by accumulation of LNCs in these membrane openings together with possible adsorption by minor LNC–membrane interactions (Van der Bruggen and Vandecasteele, 2001).

3.4. Tangential flow filtration

The large dialysis external volume did not allow detection of the LNCs that possibly passed through the membranes. Therefore, TFF with comparable membrane material (polyethersulfone) and MWCO selection was applied in order to verify whether the LNCs penetrated the membranes intact or not. Collection of small (5 mL) filtrate fractions enabled direct analysis by PCS. Fluorescence intensity of the fractions was also measured.

No original LNCs were observed from the filtrate of the 3 kDa MWCO capsule whatever the LNC size was. Instead, aggregated/decomposed material in the form of big particles and small species could be observed. *PdI*s of every fraction indicated highly heterogeneous size distributions (*PdI* = 1). Compared to dialysis, probably the applied transmembrane pressure (10–20 psi) in TFF provoked more stress towards LNCs on/inside the membrane leading to destabilization of the LNC structure. When the membrane MWCO was increased (10 kDa), initial sizes were found in the filtrate: 27–37 nm for LNC 25 nm, 50–52 nm for LNC 50 nm, and 105–140 nm for LNC 100 nm. Size distribution of the filtrated LNC 25 nm was broader (*PdI* 0.30–0.60) than those of LNC 50 nm (*PdI* 0.01–0.08) and LNC 100 nm (*PdI* 0.07–0.13) as if the LNC 25 nm dispersion aggregated slightly during the membrane passing. Instead, sizes and *PdI*s of 50 nm and 100 nm were comparable to the initial values presented in Table 3. Aggregation tendency of LNC 25 nm might have resulted either from their higher quantity in the process (same mg/mL concentration used for all sizes), higher total surface area, or higher amount of smaller particles that can penetrate the pores simultaneously (increased probability for collisions).

DCR from the PCS analysis and fluorescence intensities of the 10 kDa TFF filtrate fractions were calculated/measured in order to evaluate the concentration of LNCs in the filtrate with respect to

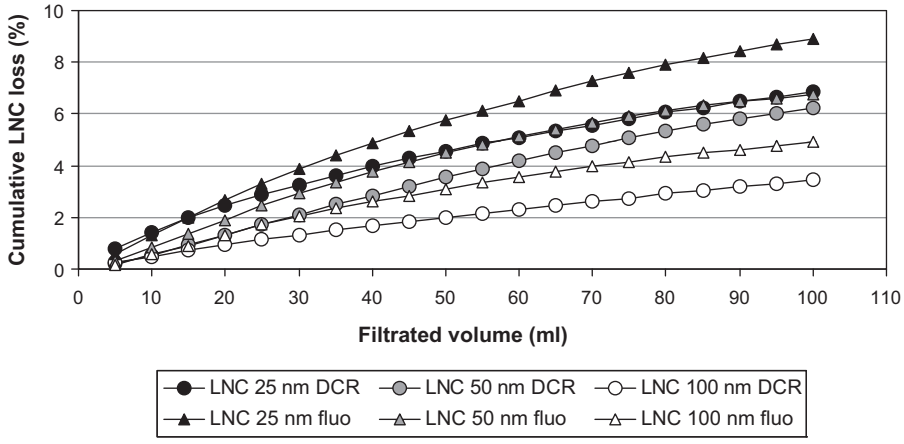

Fig. 5. Cumulative loss of LNCs during TFF with MWCO 10 kDa membrane. Each fraction was 5 mL; the results characterise the filtrated volume from 5 to 100 mL.

the initial LNC concentration. Cumulative LNC losses are presented in Fig. 5. Regardless the LNC size, the LNC loss decreased with filtrated volume. In TFF, material penetration decreases during the filtration cycle due to the membrane fouling and concentration-polarization (Li et al., 1998; Van der Meeren et al., 2004). Regardless the particle size, the cumulative LNC loss was slightly higher by the fluorescence intensity technique compared to the DCR technique. However, the loss-% proposed by the two techniques were of the same order. The highest LNC concentrations were found in the first fractions of LNC 25 nm (0.6% (fluo) or 0.8% (DCR)/fraction in the beginning; ~0.2% at 100 mL), resulting also to the highest particle loss (6.9% (DCR) or 9.0% (fluo)) at the end. Obviously, the smallest LNCs penetrated the most efficiently the membrane before eventual fouling. Concentrations/fraction of the biggest LNC 100 nm were the lowest (less than ~0.1–0.25%) together with the lowest LNC loss (3.5% (DCR) or 4.9% (fluo)) at the end. LNC 50 nm cumulative loss was 6.2% (DCR) or 6.8% (fluo) and the fractions contained ~0.2–0.4% of the initial LNCs. As a comparison, studies with (solid, non-deformable) gold nanoparticles have demonstrated that as much as 50% of 3 nm nanoparticles passed through a 70 kDa TFF membrane (Sweeney et al., 2006). In addition, the same study showed that a 10 kDa TFF membrane could decrease size and polydispersity of a 2.5 nm gold nanoparticle dispersion indicating, again, passage of nanoparticles.

Based on these TFF findings (same size and size distribution on both sides of the membrane; similar particle loss when measured by the particles themselves (DCR) or by their payload (fluorescence)), it can be assumed that the observed LNC loss resulted from membrane passing of intact LNCs rather than from decomposition of LNCs followed by formation of new particulate structures on the other side of the membrane. Overall, the more logical results of TFF were contradictory to the dialysis results where the loss of LNCs increased with particle size. In the case of dialysis, as expected earlier, majority of the LNC loss might have resulted from the accumulation of LNCs to the membrane structure. In general, these TFF results supported the assumption that LNCs can penetrate pores smaller than their diameter by deformation, and find their original shape after the passing. Also, the drop tensiometer results were in line with this: LNCs are deformable but stable.

In order to transfer these deformability observations into biological environment, an appropriate experimental setup combining biological conditions and control of membrane properties (*e.g.* pore size) should be established. A potential approach for this could be for example phospholipid-based artificial membranes (Flaten et al., 2006).

4. Conclusions

In this study, rheological properties of oil–water interface mimicking surface structure of LNCs were assessed by drop tensiometer technique. Behaviour of LNCs during purification processes was evaluated by dialysis and TFF. The aim was to evaluate if LNCs with a size of 25–100 nm can pass through membranes by deformation. Elastic nature of interfaces representing LNCs could be characterized by drop tensiometer. When changing proportions of the surfactants Lipoid® and Solutol® used in the LNC preparation, this technique enabled detection of a region where formation of stable nanocapsules is possible. The results also suggested decreasing surface deformability of LNCs with increase in their diameter. Dialysis results showed that up to 10% of LNCs can be lost during the process (*e.g.* membrane accumulation) but no clear evidence of the membrane passing was observed. Instead, LNCs with initial size properties could be found in the TFF filtrate although MWCO of the membrane used was smaller that the LNC diameter. In summary, the results support previous findings about the elastic nature of LNCs. This elastic behaviour obviously contributed to the LNC loss during purification processes, of which at least a part seemed to be caused by membrane passing by deformation. Our findings from the drop tensiometer study suggested that this technique could be a useful preliminary evaluation tool in the biodistribution and toxicology studies of semi-solid nanoparticles such as liposomes.

Acknowledgements

This work was supported by the French National Research Agency (ANR) in the frame of its programme in Nanosciences and Nanotechnologies (CALIF project no. ANR-08-NANO-006). Ms. Johanna Gutensohn is acknowledged for technical assistance.

References

Allard, E., Hindre, F., Passirani, C., Lemaire, L., Lepareur, N., Noiret, N., Menei, P., Benoit, J.P., 2008. Re-188-loaded lipid nanocapsules as a promising radiopharmaceutical carrier for internal radiotherapy of malignant gliomas. Eur. J. Nucl. Med. Mol. Imaging 35, 1838–1846.

Anton, N., Saulnier, P., Boury, F., Foussard, F., Benoit, J.-P., Proust, J.E., 2007. The influence of headgroup structure and fatty acyl chain saturation of phospholipids on monolayer behavior: a comparative rheological study. Chem. Phys. Lipids 150, 167–175.

Arkhangelsky, E., Gitis, V., 2008. Effect of transmembrane pressure on rejection of viruses by ultrafiltration membranes. Separ. Purif. Technol. 62, 619–628.

Arkhangelsky, E., Sefi, Y., Hajaj, B., Rothenberg, G., Gitis, V., 2011. Kinetics and mechanism of plasmid DNA penetration through nanopores. J. Membr. Sci. 371, 45–51.

Benjamins, J., Cagna, A., Lucassen-Reynders, E.H., 1996. Viscoelastic properties of triacylglycerol/water interfaces covered by proteins. Colloid Surf. A 114, 245–254.

Christian, D.A., Cai, S., Garbuzenko, O.B., Harada, T., Zajac, A.L., Minko, T., Discher, D.E., 2009. Flexible filaments for *in vivo* imaging and delivery: persistent circulation of filomicelles opens the dosage window for sustained tumor shrinkage. Mol. Pharm. 6, 1343–1352.

Cirpanli, Y., Allard, E., Passirani, C., Bilensoy, E., Lemaire, L., Calis, S., Benoit, J.-P., 2011. Antitumoral activity of camptothecin-loaded nanoparticles in 9L rat glioma model. Int. J. Pharm. 403, 201–206.

Dalwadi, G., Benson, H., Chen, Y., 2005. Comparison of diafiltration and tangential flow filtration for purification of nanoparticle suspensions. Pharm. Res. 22, 2152–2162.

Dalwadi, G., Sunderland, V.B., 2007. Purification of PEGylated nanoparticles using tangential flow filtration (TFF). Drug Dev. Ind. Pharm. 33, 1030–1039.

Dalwadi, G., Sunderland, B., 2008. Comparison and validation of drug loading parameters of PEGylated nanoparticles purified by a diafiltration centrifugal device and tangential flow filtration. Drug Dev. Ind. Pharm. 34, 1331–1342.

de Jaeghere, F., Allémann, E., Leroux, J.-C., Stevels, W., Feijen, J., Doelker, E., Gurny, R., 1999. Formulation and lyoprotection of poly(lactic acid-*co*-ethylene oxide) nanoparticles: influence on physical stability and *in vitro* cell uptake. Pharm. Res. 16, 859–866.

Decuzzi, P., Godin, B., Tanaka, T., Lee, S.Y., Chiappini, C., Liu, X., Ferrari, M., 2010. Size and shape effects in the biodistribution of intravascularly injected particles. J. Control. Release 141, 320–327.

Elsaesser, A., Howard, C.V., 2012. Toxicology of nanoparticles. Adv. Drug Deliv. Rev. 64, 129–137.

Farokhzad, O.C., Langer, R., 2009. Impact of nanotechnology on drug delivery. ACS Nano 3, 16–20.

Flaten, G.E., Dhanikula, A.B., Luthman, K., Brandl, M., 2006. Drug permeability across a phospholipid vesicle based barrier: a novel approach for studying passive diffusion. Eur. J. Pharm. Sci. 27, 80–90.

Heurtault, B., Saulnier, P., Benoit, J.P., Proust, J.E., Pech, B., Joel, R., 2001. Lipid nanocapsules, preparation method and use as medicine. Int. Patent WO0164328 (A1).

Heurtault, B., Saulnier, P., Pech, B., Proust, J.-E., Benoit, J.-P., 2002a. A novel phase inversion-based process for the preparation of lipid nanocarriers. Pharm. Res. 19, 875–880.

Heurtault, B., Saulnier, P., Pech, B., Proust, J.E., Benoit, J.P., 2002b. Properties of polyethylene glycol 660 12-hydroxy stearate at a triglyceride/water interface. Int. J. Pharm. 242, 167–170.

Heurtault, B., Saulnier, P., Pech, B., Benoit, J.P., Proust, J.E., 2003a. Interfacial stability of lipid nanocapsules. Colloid Surf. B 30, 225–235.

Heurtault, B., Saulnier, P., Pech, B., Venier-Julienne, M.-C., Proust, J.-E., Phan-Tan-Luu, R., Benoit, J.-P., 2003b. The influence of lipid nanocapsule composition on their size distribution. Eur. J. Pharm. Sci. 18, 55–61.

Hirsjärvi, S., Passirani, C., Benoit, J.-P., 2011. Passive and active tumour targeting with nanocarriers. Curr. Drug Discov. Technol. 8, 188–196.

Hirsjärvi, S., Peltonen, L., Hirvonen, J., 2009. Effect of sugars, surfactant, and tangential flow filtration on the freeze-drying of poly(lactic acid) nanoparticles. AAPS PharmSciTech. 10, 488–494.

Hirsjärvi, S., Qiao, Y., Royère, A., Bibette, J., Benoit, J.-P., 2010. Layer-by-layer surface modification of lipid nanocapsules. Eur. J. Pharm. Biopharm. 76, 200–207.

Kazakov, V.N., Fainerman, V.B., Kondratenko, P.G., Elin, A.F., Sinyachenko, O.V., Miller, R., 2008. Dilational rheology of serum albumin and blood serum solutions as studied by oscillating drop tensiometry. Colloid Surf. B 62, 77–82.
Kumari, A., Yadav, S.K., Yadav, S.C., 2010. Biodegradable polymeric nanoparticles based drug delivery systems. Colloid Surf. B 75, 1–18.
Lacoeuille, F., Hindré, F., Moal, F., Roux, J., Passirani, C., Couturier, O., Cales, P., Le Jeune, J.J., Lamprecht, A., Benoit, J.P., 2007. In vivo evaluation of lipid nanocapsules as a promising colloidal carrier for paclitaxel. Int. J. Pharm. 344, 143–149.
Lamprecht, A., Saumet, J.-L., Roux, J., Benoit, J.-P., 2004. Lipid nanocarriers as drug delivery system for ibuprofen in pain treatment. Int. J. Pharm. 278, 407–414.
Li, H., Fane, A.G., Coster, H.G.L., Vigneswaran, S., 1998. Direct observation of particle deposition on the membrane surface during crossflow microfiltration. J. Membr. Sci. 149, 83–97.
Li, J.B., Kretzschmar, G., Miller, R., Möhwald, H., 1999. Viscoelasticity of phospholipid layers at different fluid interfaces. Colloid Surf. A 149, 491–497.
Limayem, I., Charcosset, C., Fessi, H., 2004. Purification of nanoparticle suspensions by a concentration/diafiltration process. Sep. Purif. Technol. 38, 1–9.
Liu, L., Zhao, Q., Liu, T., Zhao, M., 2011. Dynamic surface pressure and dilatational viscoelasticity of sodium caseinate/xanthan gum mixtures at the oil–water interface. Food Hydrocolloids 25, 921–927.
Longmire, M.R., Ogawa, M., Choyke, P.L., Kobayashi, H., 2011. Biologically optimized nanosized molecules and particles: more than just size. Bioconjug. Chem. 22, 993–1000.
Minkov, I., Ivanova, T., Panaiotov, I., Proust, J., Saulnier, P., 2005a. Reorganization of lipid nanocapsules at air–water interface. I. Kinetics of surface film formation. Colloid Surf. B 45, 14–23.
Minkov, I., Ivanova, T., Panaiotov, I., Proust, J., Saulnier, P., 2005b. Reorganization of lipid nanocapsules at air–water interface. Part 2. Properties of the formed surface film. Colloid Surf. B 44, 197–203.
Morille, M., Montier, T., Legras, P., Carmoy, N., Brodin, P., Pitard, B., Benoit, J.-P., Passirani, C., 2010. Long-circulating DNA lipid nanocapsules as new vector for passive tumor targeting. Biomaterials 31, 321–329.
Morille, M., Passirani, C., Dufort, S., Bastiat, G., Pitard, B., Coll, J.-L., Benoit, J.-P., 2011. Tumor transfection after systemic injection of DNA lipid nanocapsules. Biomaterials 32, 2327–2333.
Müller, R.H., Shegokar, R., Keck, C.M., 2011. 20 years of lipid nanoparticles (SLN & NLC): present state of development & industrial applications. Curr. Drug Discov. Technol. 8, 207–227.
Paillard, A., Hindré, F., Vignes-Colombeix, C., Benoit, J.-P., Garcion, E., 2010. The importance of endo-lysosomal escape with lipid nanocapsules for drug subcellular bioavailability. Biomaterials 31, 7542–7554.
Peltier, S., Oger, J.-M., Lagarce, F., Couet, W., Benoit, J.-P., 2006. Enhanced oral paclitaxel bioavailability after administration of paclitaxel-loaded lipid nanocapsules. Pharm. Res. 23, 1243–1250.
Perry, J.L., Herlihy, K.P., Napier, M.E., DeSimone, J.M., 2011. PRINT: a novel platform towards shape and size specific nanoparticle theranostics. Acc. Chem. Res. 44, 990–998.
Ramírez, P., Pérez, L.M., Trujillo, L.A., Ruiz, M., Muñoz, J., Miller, R., 2011. Equilibrium and surface rheology of two polyoxyethylene surfactants (CiEOj) differing in the number of oxyethylene groups. Colloid Surf. A 375, 130–135.
Roger, E., Lagarce, F., Garcion, E., Benoit, J.P., 2009. Lipid nanocarriers improve paclitaxel transport throughout human intestinal epithelial cells by using vesicle-mediated transcytosis. J. Control. Release 140, 174–181.
Saez, A., Guzmán, M., Molpeceres, J., Aberturas, M.R., 2000. Freeze-drying of polycaprolactone and poly(D,L-lactic-glycolic) nanoparticles induce minor particle size changes affecting the oral pharmacokinetics of loaded drugs. Eur. J. Pharm. Biopharm. 50, 379–387.
Sakai, K., 1994. Determination of pore size and pore size distribution. 2. Dialysis membranes. J. Membr. Sci. 96, 91–130.
Santini, E., Liggieri, L., Sacca, L., Clausse, D., Ravera, F., 2007. Interfacial rheology of Span 80 adsorbed layers at paraffin oil–water interface and correlation with the corresponding emulsion properties. Colloid Surf. A 309, 270–279.
Saulnier, P., Boury, F., Malzert, A., Heurtault, B., Ivanova, T., Cagna, A., Panaïotov, I., Proust, J.E., 2001. Rheological model for the study of dilational properties of monolayers. Comportment of dipalmitoylphosphatidylcholine (DPPC) at the dichloromethane (DCM)/water interface under ramp type or sinusoidal perturbations. Langmuir 17, 8104–8111.
Sweeney, S.F., Woehrle, G.H., Hutchison, J.E., 2006. Rapid purification and size separation of gold nanoparticles via diafiltration. J. Am. Chem. Soc. 128, 3190–3197.
Torchilin, V., 2007. Micellar nanocarriers: pharmaceutical perspectives. Pharm. Res. 24, 1–16.
Torchilin, V.P., 2005. Recent advances with liposomes as pharmaceutical carriers. Nat. Rev. Drug Discov. 4, 145–160.
Urase, T., Yamamoto, K., Ohgaki, S., 1996. Effect of pore structure of membranes and module configuration on virus retention. J. Membr. Sci. 115, 21–29.
Van der Bruggen, B., Vandecasteele, C., 2001. Flux decline during nanofiltration of organic components in aqueous solution. Environ. Sci. Technol. 35, 3535–3540.
Van der Meeren, P., Saveyn, H., Bogale Kassa, S., Doyen, W., Leysen, R., 2004. Colloid-membrane interaction effects on flux decline during cross-flow ultrafiltration of colloidal silica on semi-ceramic membranes. Phys. Chem. Chem. Phys. 6, 1408–1412.
Vanpouille-Box, C., Lacoeuille, F., Belloche, C., Lepareur, N., Lemaire, L., LeJeune, J.-J., Benoit, J.-P., Menei, P., Couturier, O.F., Garcion, E., Hindré, F., 2011a. Tumor eradication in rat glioma and bypass of immunosuppressive barriers using internal radiation with 188Re-lipid nanocapsules. Biomaterials 32, 6781–6790.
Vanpouille-Box, C., Lacoeuille, F., Roux, J., Aubé, C., Garcion, E., Lepareur, N., Oberti, F., Bouchet, F., Noiret, N., Garin, E., Benoit, J.-P., Couturier, O., Hindré, F., 2011b. Lipid nanocapsules loaded with rhenium-188 reduce tumor progression in a rat hepatocellular carcinoma model. PLoS ONE 6, e16926.
Vonarbourg, A., Passirani, C., Saulnier, P., Benoit, J.-P., 2006a. Parameters influencing the stealthiness of colloidal drug delivery systems. Biomaterials 27, 4356–4373.
Vonarbourg, A., Passirani, C., Saulnier, P., Simard, P., Leroux, J.-C., Benoît, J.P., 2006b. Evaluation of pegylated lipid nanocapsules versus complement system activation and macrophage uptake. J. Biomed. Mater. Res. A 78A, 620–628.
Vonarbourg, A., Saulnier, P., Passirani, C., Benoit, J.-P., 2005. Electrokinetic properties of noncharged lipid nanocapsules: influence of the dipolar distribution at the interface. Electrophoresis 26, 2066–2075.
Wüstneck, R., Moser, B., Muschiolik, G., 1999a. Interfacial dilational behaviour of adsorbed β-lactoglobulin layers at the different fluid interfaces. Colloid Surf. B 15, 263–273.
Wüstneck, R., Wüstneck, N., Grigoriev, D.O., Pison, U., Miller, R., 1999b. Stress relaxation behaviour of dipalmitoyl phosphatidylcholine monolayers spread on the surface of a pendant drop. Colloid Surf. B 15, 275–288.
Zou, J., Saulnier, P., Perrier, T., Zhang, Y., Manninen, T., Toppila, E., Pyykkö, I., 2008. Distribution of lipid nanocapsules in different cochlear cell populations after round window membrane permeation. J. Biomed. Mater. Res. B 87B, 10–18.
Zydney, A.L., Xenopoulos, A., 2007. Improving dextran tests for ultrafiltration membranes: effect of device format. J. Membr. Sci. 291, 180–190.